Accumulated metagenomic studies reveal recent migration, whole genome evolution, and taxonomic incompleteness of orthomyxoviruses

Gytis Dudas[a,1] **and Joshua Batson**[b,1]

[a]Institute of Biotechnology, Life Sciences Centre at Vilnius University, Vilnius, Lithuania, [b]Chan Zuckerberg Biohub, San Francisco CA, USA, [1]Corresponding authors: gytis.dudas@gmc.vu.lt, joshua.batson@gmail.com

August 31, 2022

Abstract

Metagenomic studies have uncovered an abundance of novel viruses by looking beyond hosts of obvious public health or economic interest. The discovery of conserved genes in viruses infecting geographically and phylogenetically diverse hosts has provided important evolutionary context for human and animal pathogens. However, the resulting viral genomes are often incomplete, and analyses largely characterize the distribution of viruses over their dynamics. Here, we show how the accumulated data of metagenomic studies can be integrated to reveal geographic and evolutionary dynamics in a case study of *Orthomyxoviridae*, the family of RNA viruses containing influenza. First, we use sequences of the orthomyxovirus Wuhan mosquito virus 6 to track the global migrations of its host. We then look at overall orthomyxovirus genome evolution, finding significant gene gain and loss across the family, especially in the surface proteins responsible for cell and host tropism. We find that the surface protein of Wuhan mosquito virus 6 exhibits accelerated non-synonymous evolution suggestive of antigenic evolution, and an entire quaranjavirus group bearing highly diverged surface proteins. Finally we quantify the progress of orthomyxovirus discovery and forecast that many highly diverged *Orthomyxoviridae* remain to be found. We argue that continued metagenomic studies will be fruitful for understanding the dynamics, evolution, ecology of viruses and their hosts, regardless of whether novel species are actually identified or not, as long as study designs allowing for the resolution of complete viral genomes are employed.

Summary

The number of known virus species has increased dramatically through metagenomic studies, which search genetic material sampled from a host for viral genes. Here, we focus on an important viral family with over a hundred recently discovered species infecting hosts from humans to fish. We find one virus, discovered in mosquitoes in China, recently spread across the globe. Surface proteins used to enter cells show signs of rapid evolution in that virus and across the family. We compute the rate at which new species discovered add evolutionary history to the tree of life, predict that many viruses remain to be discovered, and discuss what appropriately designed future studies can teach us about how diseases cross between continents and species.

Viruses that cause disease in humans and economically important organisms were the first to be isolated and characterized. Recently, cheap DNA sequencing has enabled a wave of metagenomic studies in a broader range of hosts, in which viruses are identified in a host sample by nucleic acid sequence alone and a new viral species is said to be discovered if that sequence is sufficiently diverged. As a result, the number of known viral species has increased by more than an order of magnitude in the decade since 2012 (Roux et al., 2021). While some entirely new viral families have been discovered, many of these new species are interleaved on the tree of life with viruses infecting hosts of economic importance. Studying their ecology (Shi et al., 2019) and host associations (Li et al., 2015; Shi et al., 2018) provides insight into the host-switching and genome evolution processes important for the evolution of pathogenicity.

This richer tree has provided some early success stories, such as jingmenviruses first discovered metagenomically in ticks (Qin et al., 2014) and later identified as causing human disease (Wang et al., 2019). Surveillance in hosts known to pose disproportionate risk, such as bats, (Ge et al., 2016) has provided context for zoonotic pathogens like SARS-CoV-2 (Wu et al., 2020). Metagenomic studies carried out at scale can effectively multiplex other tasks previously addressed with targeted sampling, like understanding the evolutionary history of human pathogens (Keele et al., 2006) or using viruses that evolve faster than their hosts to track host movements (Wheeler et al., 2010).

Here, we seek to show how accumulated data from metagenomic studies can provide deep insights into viral evolution and dispersion across a family through a case study of *Orthomyxoviridae*. *Orthomyxoviridae* are a family of enveloped segmented negative sense single-stranded RNA viruses that infect vertebrates and arthropods. Orthomyxovirus discovery has historically been driven by impact on human health (*e.g.* influenza virus) and livelihood (*e.g.* salmon infectious anemia virus), or association with known disease vectors (*e.g.* the tick-borne Johnston Atoll quaranja- and Thogotoviruses). The metagenomic revolution has resulted in ten times more orthomyxovirus species being discovered over the last decade than in the previous 79 years since the first orthomyxovirus discovery, of influenza A, in 1933. The vast majority of known orthomyxoviruses use one of two surface protein classes, with vertebrate-infecting-only members (influenza, isaviruses) using one or more class I membrane fusion proteins derived from hemagglutinin-esterase-fusion (HEF) (Parry et al., 2020), sometimes delegating the esterase function to a separate protein neuraminidase (NA), and arthropod-infecting ones (quaranja- and thogotovirus, which sometimes spill over into vertebrates) using a class III membrane fusion protein called gp64 (Garry and Garry, 2008). The number of segments of orthomyxoviruses with genomes known to be complete varies from 6 to 8, but many metagenomically discovered viruses have a smaller number of segments characterized, or only the polymerase. To our knowledge, an inventory of surface protein class use and segment content of *Orthomyxoviridae* is not yet available.

We start by showing how closely related virus sequences observed across numerous studies can reveal host spatial dynamics and virus microevolution, using the orthomyxovirus Wuhan mosquito virus 6 (WMV6). We then map out known genome composition across *Orthomyxoviridae*, highlighting parts of the tree where changes to segment numbers are likely to have taken place. In looking at genome composition we pay close attention to surface protein use, and focus particularly on gp64 proteins used by

thogoto- and quaranjaviruses. We find surface proteins to be quite mobile within *Orthomyxoviridae* over evolutionary timescales and identify a clade of quaranjaviruses known to have acquired new segments using distinctly diverged gp64 proteins. Finally we borrow methods from macroevolutionary research to quantitatively assess the pace at which orthomyxovirus evolutionary history is being uncovered, finding that despite their already transformative effect, metagenomic discovery efforts are likely to continue to find substantially diverged members of *Orthomyxoviridae* for some time.

1 Results

1.1 Insect virus population dynamics

Wuhan mosquito virus 6 (WMV6), a mosquito orthomyxovirus seen frequently across much of the world (Pettersson et al., 2019; Li et al., 2015; Shi et al., 2017) belongs to a quaranjavirus clade that has two extra segments compared to other quaranjaviruses (Batson et al., 2021). We inferred the reassortment network (Müller et al., 2020) of currently available WMV6 sequence data to infer the relationships between segments, their reassortments with respect to each other and timings of both (Fig. 1A and Supp. Fig. 1). We find that all WMV6 segments share a common ancestor within the last 60-odd years, which is not unusual for insect viruses (Webster et al., 2015) (Fig. 1A and Supp. Figs. 2 and 3), and that a more recent, potentially global, sweep is underway, with segments from four continents sharing a common ancestor in the last 20 years (Fig. 1B).

Although the geographic population structure of WMV6 is appreciable, with samples from the same country often close on the tree, reassortment events indicate contact between genomic lineages across vast distances. For example, reassortment events #2 and #3 in Fig. 1A indicate contact as recently as 2010-2015 between WMV6 lineages eventually found in Australia and California. Similarly, some lineages found in China are related to recent (*circa* 2017) Californian lineages (reassortment event #1 in Fig. 1A). Even lineages not represented in the reassortment network due to incomplete genomes show evidence of gene flow, like Chinese and Greek PB1 sequences in Fig. 1B. These results indicate that WMV6 populations are very mobile.

1.2 Surface protein evolution within *Orthomyxoviridae*

We find gp64, the presumed surface protein of WMV6, is evolving faster in terms of non-synonymous substitutions per codon per year than the rest of the WMV6 genome, save for the smallest segment, which is expected to be spliced (hypothetical3 (Batson et al., 2021)) and therefore likely to contain overlapping reading frames (Fig. 2A and Supp. Fig. 4). The rate of non-synonymous evolution in WMV6 gp64 is also faster than the spike protein of endemic human coronaviruses (Kistler and Bedford, 2021) and about as fast as Ebola virus glycoprotein GP during the West African epidemic (Park et al., 2015)(Fig. 2A), with highest dN/dS values concentrated around its fusion loops (Garry and Garry, 2008) (Supp. Fig. 5). We see elevated rates of amino acid evolution in gp64 across the wider clade defined by Astopletus and Ūsinis viruses, to which WMV6 belongs. Members have PB1 proteins (encoding RdRp) closely related (Fig. 2B) but gp64 proteins substantially diverged from other quaranjaviruses and each other (Fig. 2C and Supp. Fig. 6). The pronounced non-synonymous divergence in gp64 at the WMV6 population level and the wider Asto-Ūsinis clade level indicates some

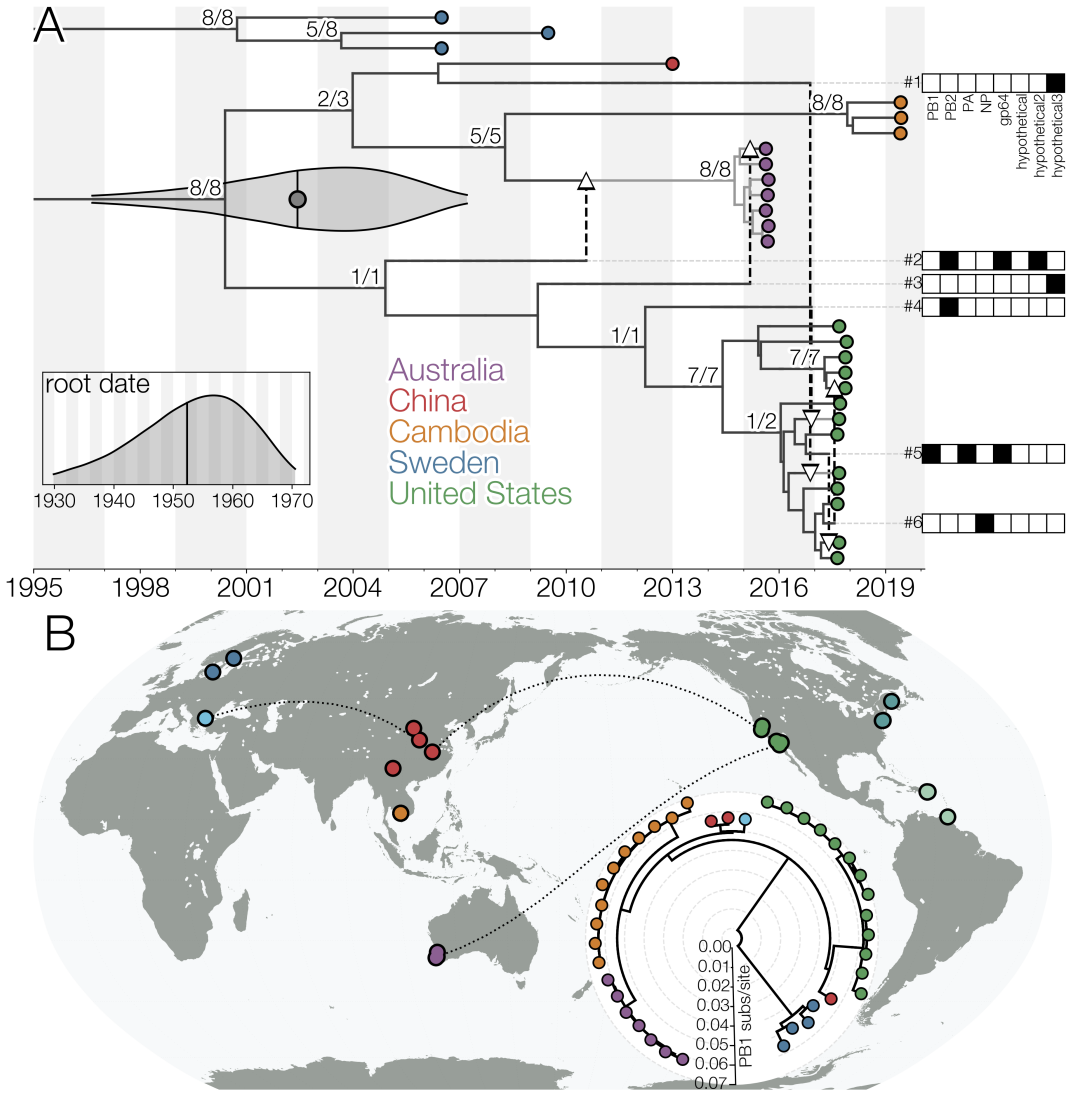

Figure 1. A) Reassortment network of full WMV6 genomes. Tips are indicated with circles and colored based on location. Reassortant edges are indicated with dashed lines, numbered with segments carried along the edge indicated with filled-in rectangles to the right of the plot (for clearer segment embeddings see Supp. Fig. 1). The network is truncated to 1995 with a violin plot indicating the 95% highest posterior density for the date of the common ancestor of non-Swedish WMV6 samples. Black vertical line with the gray dot within the violin plot indicates the mean estimate. The inset plot indicates same for the root date of the network with black vertical line indicating the mean. Since the summary procedure for the posterior distribution of networks is overly conservative (see Supp. Fig. 2), node supports are expressed as number of times a given node is seen with $\geq$0.95 probability in segment embedding summary trees, after carrying out the subtree prune-regraft procedures for any given embedding indicated by reassortant edges, out of all such nodes. B) A maximum likelihood (ML) tree of WMV6 PB1 sequences, showing additional samples for which full genomes were not available, as well as the sampling locations of all WMV6 sequences. Dotted lines connect locations that have experienced recent WMV6 gene flow based on reassortment patterns. For all available WMV6 segment data see Supp. Fig. 3.

evolutionary pressure on this surface protein, such as diversifying selection pressure from repeat infections of hosts with humoral immune systems.

The paucity of sequenced gp64 proteins related to those of the Asto-Ūsinis clade highlights the poor state of knowledge of genome composition across *Orthomyxoviridae*. The closest relative with reliable segment information (based on EM photographs (Allison et al., 2015)) is the genus *Quaranjavirus* with seven segments (Fig. 2B), indicating that since the common ancestor of the *Quaranjavirus* genus and the Asto-Ūsinis clade, segments were either lost in the former or gained in the latter. Such gaps (Fig. 2B) in understanding seem to increase with phylogenetic distance from vertebrate-pathogenic viruses, a hallmark of retrospective research into outbreaks rather than prospective efforts aimed at understanding the correlates of pathogenicity across this family.

We also observe plasticity in orthomyxovirus genome composition — regardless of rooting, the PB1 tree requires at least two switches in viral membrane fusion protein class to explain the current distribution of HEF-like (class I) and gp64-like (class III) proteins. Even within gp64-using orthomyxoviruses changes between different gp64 lineages are apparent, *e.g.* Hubei orthomyxo-like virus 2 carries gp64 related to the Asto-Ūsinis clade yet does not belong to it in PB1 (Fig. 2B and Supp. Fig. 6). Almost all orthomyxoviruses use either HEF-like or gp64-like proteins, with Rainbow / Steelhead trout orthomyxoviruses (and one additional relative (Batts et al., 2017), not shown) being the only exceptions. Both clearly possesses an influenza A/B-like neuraminidase (NA) but the protein termed "hemagglutinin" (Batts et al., 2017) does not resemble any known protein (Finn et al., 2011). While *Orthomyxoviridae* are a moderately-sized virus family, they make use of a diverse and evolving set of surface proteins.

1.3 Discovery of phylogenetic diversity

We now analyse the progress made by virus discovery studies on *Orthomyxoviridae*. There are two clear phases: before 2015, public health investigations of pathogens infecting humans and farmed animals or vectored by ticks led to the discovery of 14 viruses. Since 2015, when lower costs of sequencing enabled large metagenomic surveys in arthopods and vertebrates of little immediate economic value (Li et al., 2015; Shi et al., 2018), 115 additional viruses have been discovered (Supp. Fig. 7).

To quantify how each discovery contributed to our knowledge of the family's evolutionary history, we take a phylogenetic approach, building a maximum-likelihood tree of the sole protein shared by all RNA viruses, RNA-dependent RNA polymerase (RdRp) (Koonin and Dolja, 2014), encoded here in the PB1 gene (Kobayashi et al., 1996) (Fig. 3A). We scan through the tree based on the chronology of discovery, attributing to each species the sum of the lengths of the branches ancestral to that species but not to earlier species. This quantity is called the phylogenetic diversity (PD), a metric commonly used in ecology and macroevolution (Lum et al., 2022), and represents the amount of independent evolution (Felsenstein, 1985) contributed by a species to a tree.

We find that distinctive viruses, those contributing significant PD, have continued to be discovered each year (Fig. 3B). For example, the Wenling orthomyxo-like virus 2 found in 2018 is nearly as distinctive relative to the viruses discovered before it as the Infectious salmon anemia virus found in 1984 was. There is no correlation between the year of discovery and the maximum PD contributed by an orthomyxovirus (Spearman

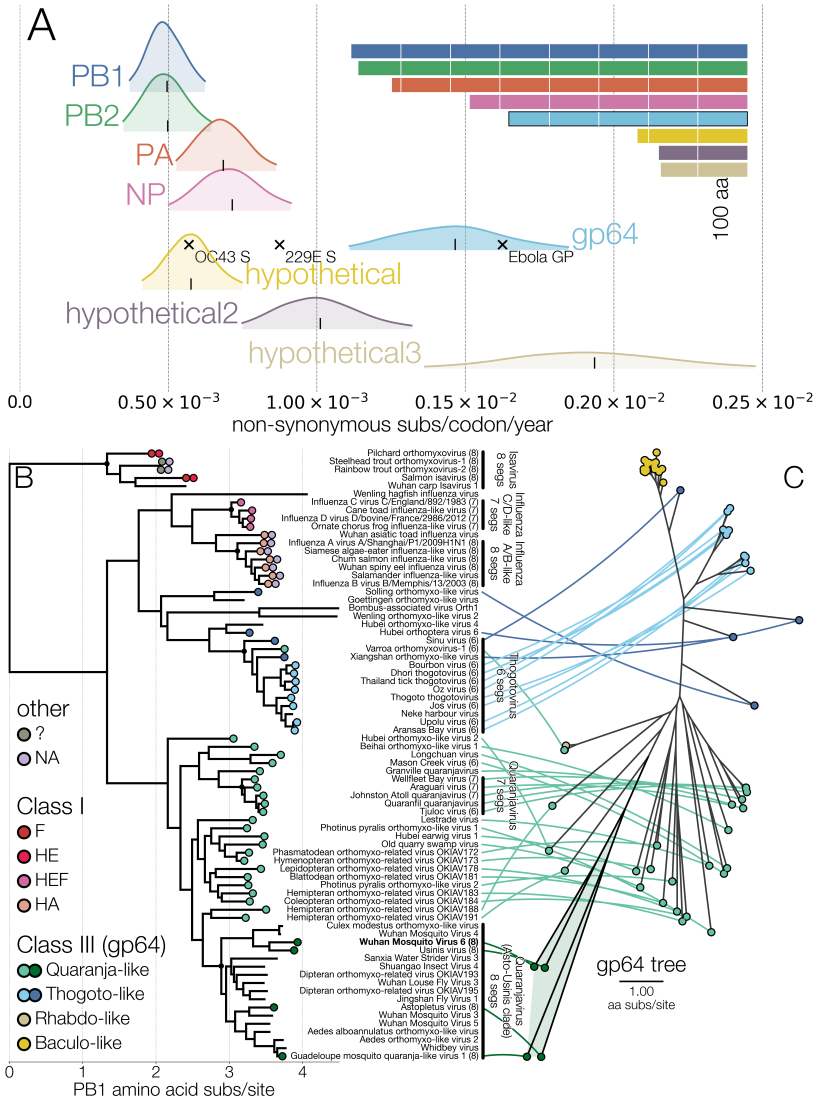

Figure 2. A) 95% highest posterior densities for the rate of non-synonymous mutations per codon per year for each known WMV6 gene (indicated by color). Black vertical ticks indicate the mean estimate, × marks similar estimates for the surface glycoprotein (GP) of Ebola virus and the surface Spike proteins (S) of human seasonal coronaviruses OC43 and 229E. The length of each open reading frame is indicated to the right, with white lines denoting 100 amino acid increments and gp64 outlined in black. Note that putative hypothetical 3 protein is expected to be the result of splicing (Batson et al., 2021) and therefore can contain overlapping coding regions where synonymous changes in one frame may be deleterious in another. B) Rooted phylogenetic tree depicts the relationships between PB1 proteins of orthomyxoviruses. Surface proteins are marked as colored circles at the tips: red hues for class I membrane fusion proteins, green/blue and yellow/brown for class III proteins (gp64) of *Orthomyxoviridae* and non-*Orthomyxoviridae*, respectively, and lilac for neuraminidases. Likely genome composition for certain groups are highlighted with black vertical lines to the right of the tree, with corresponding implied common ancestor with such organization marked with a black circle in the tree. C) An unrooted phylogeny to the right of the PB1 tree shows the relationships between gp64 proteins found in thogoto- or thogoto-like- (blue), quaranja- or quaranja-like- (green), baculo- (yellow), and some rhabdoviruses (tan). Where available, each orthomyxovirus gp64 protein is connected to its corresponding PB1 sequence. Black branches with a faded green area in the gp64 tree to the right indicate the position of Asto-Ūsinis gp64 proteins.

r = 0.02, p-value = 0.95). In contrast, the average PD contributed per species does decrease with time (Spearman r = −0.17, one-tailed p-value = 0.054/2 = 0.027), as shared evolutionary history is attributed to earlier discoveries. While the orthomyxoviruses discovered each year are, on average, less distinctive, the increased host breadth and rapid pace of current studies result in evolutionarily highly distinctive species.

Fig. 3C shows the cumulative PD of PB1 after each new orthomyxovirus discovery. Early *Orthomyxoviridae* discovery efforts do show some bias, finding viruses more related to one-another than by chance: until 2018, the empirical accumulation of PD (black dots) is mostly below the 95 percentile envelope of 1000 random permutations of discovery order (gray hatched area). We fit the empirical data with a logarithmic function ($f(x) = A \times log_2(1 + x/B)$, where A = 46.3 and B=62.4), indicated with a red line in Fig. 3C). We can extrapolate this curve into the future, *e.g.* 200th orthomyxovirus is expected to contribute ≈0.26 amino acid substitutions per site to PB1 PD (bringing total PD to 95.9), and the 500th ≈0.12 (total PD 146.8). Note that any remaining bias in the current viral discovery paradigm, leaving some parts of the *Orthomyxoviridae* tree of life undersampled, would manifest in a future PD curve higher than the extrapolation of the one observed so far. There is, regardless, an eventual limit, in which the PD gain of a new discovery is less than the threshold of difference used to define a new species (*e.g.* 0.1 aa sub/site would currently be reached around the 600th species). If current trends continue, there would remain at least hundreds of additional species to be discovered.

2 Discussion

In this work, we endeavored to show how the accumulation of metagenomic data can lead to a new stage in viral studies. We focused on the family *Orthomyxoviridae*, synthesizing data across numerous studies to analyze geographic, evolutionary, and taxonomic trends.

We first focus on a single recently discovered mosquito RNA virus - Wuhan mosquito virus 6 (Li et al., 2015) (WMV6) - whose frequency and fast evolution uniquely enable the tracking of mosquito populations. WMV6 has rapidly disseminated across vast distances, and while anthropogenic (shipping, air travel) (Lounibos, 2002; Fonseca et al., 2006; Bataille et al., 2009) or abiotic (windborne migration) (Huestis et al., 2019) mechanisms may contribute, the virus' extremely diverged and actively diversifying gp64 surface proteins suggest a potential vertebrate host. Indeed, the rapid sweep of the USA by West Nile virus was accelerated by the movement of both its mosquito vector and its diverse avian hosts (Di Giallonardo et al., 2015). While alternation between vertebrate host species could theoretically produce diversifying selection on the WMV6 surface protein, gp64 uses NPC1 (Li et al., 2019), a highly conserved metazoan protein, as its receptor. We thus believe it more likely that WMV6 gp64 diversity is selected for by repeat exposure to vertebrate hosts (Jong et al., 2007), which help disperse WMV6 (Lycett et al., 2019) and reduce its effective population sizes (Bedford et al., 2011). Previously, this sort of phylodynamic analysis was limited to known human and animal pathogens (Drummond et al., 2003; Wheeler et al., 2010). As metagenomic discovery efforts continue more systems like WMV6 will undoubtedly be found, contributing to research areas outside of virus evolution, like disease vector dispersal and shifting host distributions under climate

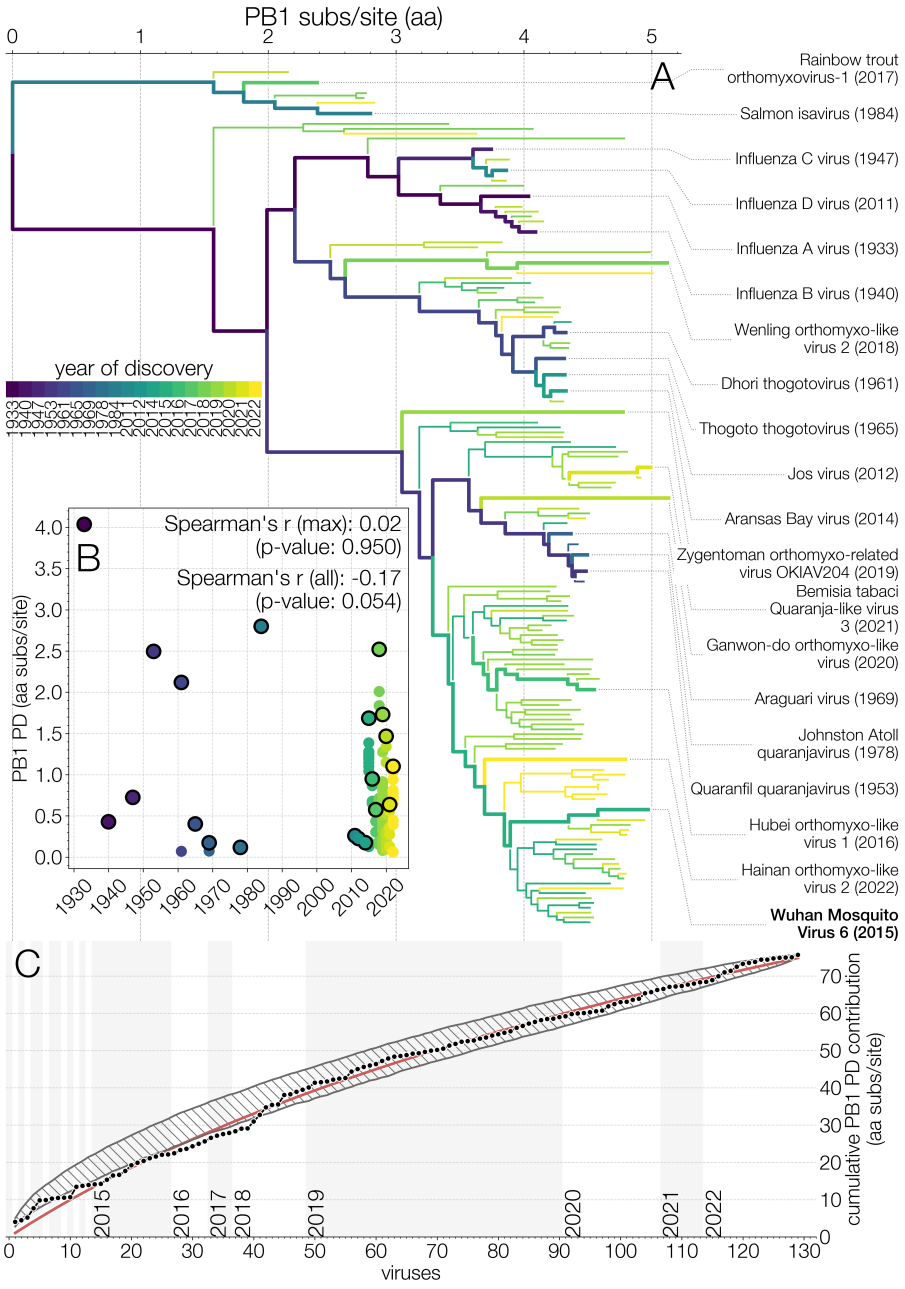

Figure 3. Discovery of *Orthomyxoviridae* PB1 phylogenetic diversity (PD). A) Maximum likelihood (ML) tree of *Orthomyxoviridae* PB1 proteins. Branch color indicates earliest discovery year of the lineage. Evolutionary history in purple branches was discovered earlier than yellow branches. Virus species contributing the most PD in their year of discovery are labelled on the right, and indicated with thicker paths in the phylogeny. B) Inset scatter plot shows PD contributions of each virus versus its year of discovery, with black outlines indicating the maximal PD contributor each year. While the average PD contribution of a newly discovered orthomyxovirus is decreasing with time (Spearman's r=-0.17, one-tailed p-value: 0.027), the PD contribution of the most novel virus discovered each year has held steady (Spearman's r=0.02, one-tailed p-value: 0.950/2=0.425). C) Cumulative PB1 PD contribution from successive orthomyxovirus discoveries (black dots) with logarithmic least-squares fit (red line). Gray hatched area indicates the 95 percentile range of cumulative PD contributions under 1000 random permutations of taxa discovery order.

change.

Zooming out, we find a highly modular and fluid genomic organization in the family *Orthomyxoviridae*. This presents an interesting conundrum – how and why are novel segments acquired so readily by orthomyxoviruses, given that packaging signals encompass multiple sites (Baker et al., 2014) and obtaining segments via recombination is hard (Chare et al., 2003)? (Splitting genomes via segmentation is better documented (Kondo et al., 2006; Qin et al., 2014) and easier to explain conceptually (Ke et al., 2013).) Observed frequent switches in surface proteins may be selected for because of their importance in determining host and tissue tropism. We may also be missing additional classes of surface protein, beyond HEF-like and gp64, because of a reliance on sequence homology for protein identification. Indeed, many pooled studies produce incomplete viral genomes, with too few segments relative to their clade, so there is a possibility that significant undetected gain and loss of segments has occurred even within already-discovered viruses. To assess such evolutionary questions will require metagenomic studies to look beyond discovering conserved genes in increasing numbers of species to completing viral genomes by sequencing individuals across geographic transects (Batson et al., 2021). Laboratory studies will be necessary to identify the functions of these novel segments and to confirm/determine tropism of discovered surface proteins (Arunkumar et al., 2021).

Finally, we assess the overall progress of orthomyxovirus discovery from the perspective of phylogenetic diversity (PD). We find that the many new species of orthomyxovirus being discovered every year are adding significant evolutionary history to the family tree. We may contrast this to the situation for birds, which have been studied and characterized for centuries and for which the discovery of new and distinctive species is now rare (Lum et al., 2022). Where the PD contribution of the most distinctive avian species discovered in each year exhibits a strong downwards trend (Lum *et al.*(Lum et al., 2022) Fig. 4), the PD of the most distinctive orthomyxovirus discovered each year remains high (our Fig. 3B). The aggregate trend also indicates that significant PD remains to be discovered: if logarithmic trend continues, known *Orthomyxoviridae* diversity would double on the discovery of the 531st member, before running into a taxonomic threshold at the species-definition barrier. (While there is a risk that some metagenomic sequence represents endogenized viral genes, this is extremely rare for the RdRp gene we use to calculate PD (Whitfield et al., 2017).) This complements the argument made by Parry et al. (2020) for the existence of many more influenza-like viruses based on virus-host codivergence and the existence of many unsampled host species. We believe that phylogenetic diversity measures, already in widespread use in ecology and macroevolution, will prove useful to the metagenomic virus discovery community as it seeks to assess ongoing progress and predict future payoff.

This work was made possible by the public sharing of annotated genomes, raw sequencing data, and sampling metadata from groups across the world. As metagenomic surveys expand across diverse hosts and geographies, the accumulation of sequence data allows a depth of analysis that moves beyond species discovery and into ecological and evolutionary dynamics; encountering new samples of previously seen viruses, instead of being seen as a disappointment, can be viewed as opportunity for more granular phylodynamic analysis. The evolutionary interdependence of sequence within and between organisms generates increasing returns on additional surveys. With appropriate study designs, good data organization, and public sharing strategies, the commu-

nity's search into the shape of the "virosphere" will offer large dividends for many fields of research.

3 Methods

3.1 Use of viruses for host tracking

Most of Wuhan mosquito virus 6 (WMV6) virus data (Chinese, Californian and Australian genomes) were derived from a previous publication (Batson et al., 2021). Assembled contigs from the Swedish study (Pettersson et al., 2019) were provided by John Pettersson while the Cambodian sequences were kindly provided by Jessica Manning, Jennifer Bohl, Dara Kong and Sreyngim Lay, where WMV6 segments described later (Batson et al., 2021) were identified by similarity.

Puerto Rican segments were recovered by mapping reads from SRA entries SRR3168916, SRR3168920, SRR3168922, and SRR3168925 (Frey et al., 2016) to segments of Californian strain CMS001_038_Ra_S22 using bwa v0.7.17 (Li and Durbin, 2009) but most segments except for NP did not have good coverage to be assembled with certainty. Greek segments were recovered by mapping reads from SRA entry SRR13450231 (Konstantinidis et al., 2021) using the same approach as described earlier. New Chinese segments from 2018 (He et al., 2021) were similarly recovered by mapping reads from China National GeneBank Sequence Archive accessions CNR0266076 and CNR0266075 using the same approach as described earlier. New Chinese and Greek segments tended to have acceptable coverage except for segments hypothetical 2 and hypothetical 3 where only individual reads could be detected.

All sequences were aligned using MAFFT (Katoh et al., 2005) and trimmed to the coding regions of each segment. PhyML v.3.3.2 was used to generate maximum likelihood phylogenies of each segment under an HKY+Γ_4 (Hasegawa et al., 1985; Yang, 1994) model. Each tree was rooted via least squares regression of tip dates against divergence from root in TreeTime (Sagulenko et al., 2018).

27 WMV6 genomes (13 from California, 7 from Australia, 3 from Cambodia, 3 from Sweden, and 1 from China) were analyzed using the reassortment network method (Müller et al., 2020) implemented in BEAST v2.6 (Bouckaert et al., 2019). For the smallest segment coding for the hypothetical 3 protein, two Ns were inserted after the 349th nucleotide from the initiation codon ATG to account for the presence of a suspected splicing site (Batson et al., 2021) that brings a substantial portion of this segment back to being coding. Each segment was partitioned into codon positions 1+2 and 3 evolving under independent HKY+Γ_4 (Hasegawa et al., 1985) models of nucleotide substitution and independent strict molecular clocks calibrated by using tip dates. By default a constant effective population size coalescent tree prior is applied to the reassortment network. Default priors were left in all cases except for effective population size (set to exponential distribution with mean at 100 years) and reassortment rate (set to exponential distribution with mean 0.001 events/branch/year) to get conservative estimates and prevent exploration of complicated parameter space. MCMC was run for 200 million states, sampling every 20000 states in triplicate, after which all chains were combined after discarding 10% of the states as burn-in and confirmed to have reached stationarity using Tracer (Rambaut et al., 2018). The reassortment network was summarized using the native BEAST v2.6 tool (ReassortmentNetworkSummarizer) provided with the package. Posterior embeddings of each segment

within the network (in the form of clonal phylogenetic trees) were summarized using TreeAnnotator v.1.10.4 after combining independent runs after discarding 10% of the states as burn-in.

In our personal experience ReassortmentNetworkSummarizer is overly conservative when summarizing reassortment networks due to reassortant edges requiring conditioning on both the origin and destination clades. As such we removed reassortant edges with $\leq$0.1 posterior support and summarized posterior supports by first extracting the embedding of each segment from the summarized network by carrying out the subtree prune-and-regraft procedures implied by reassortant edges and then finding how many of the same clades are found in posterior summaries of segment embeddings and how many of those are supported with posterior probability $\geq$0.95.

All trees were visualized using baltic (https://github.com/evogytis/baltic) and matplotlib (Hunter, 2007).

3.2 Orthomyxovirus segmentation and surface proteins

For each clonal WMV6 segment embedding within the reassortment network 1 000 trees from the posterior distribution were extracted after removing 10% burnin and combining all three independent runs. These trees were then used as empirical trees to be sampled from in a BEAST v.1.10.4 (Suchard et al., 2018) renaissance counting analysis (Lemey et al., 2012) run for 10 million states, sampling every 1 000 states. As a comparison estimates of non-synonymous evolution were computed from previously published data of seasonal human coronaviruses OC43 and 229E (Kistler and Bedford, 2021), and Ebola virus (Park et al., 2015).

Orthomyxovirus PB1 protein sequences from each genus - isa-, influenza, thogoto-, and quaranjaviruses were used as queries in a protein BLAST (Altschul et al., 1990) search with influenza A, B, C, and D viruses excluded from the search. Having identified the breadth of PB1 protein diversity and having downloaded representative PB1 proteins of influenza A, B, C, and D we aligned all sequences using MAFFT (Katoh et al., 2005) (E-INS-i mode) and removed sequences that were identical or nearly identical, as well as short or poorly aligning sequences. We repeated this procedure with blast hits to capture as much PB1 diversity as is publicly available. Partial, poorly aligning or insufficiently distinct PB1 sequences were removed from the analysis.

We used the same data gathering technique for surface proteins. To identify HEF-like proteins we used isavirus HE and influenza C and D virus HEF proteins as queries but did not identify any additional proteins. The claimed hemagglutinin proteins of Rainbow and Steelhead trout isaviruses did not resemble anything on GenBank except each other and did not produce any significant hits via HHpred (Finn et al., 2011). BLAST searches using orthomyxovirus gp64 relatives identified thogoto- and quaranjavirus surface proteins, as well as baculoviruses and rhabdoviruses with identifiably related proteins. The presumed gp64 proteins found within the clade encompassed by Ūsinis, Astopletus (discovered in California) and WMV6 with Guadeloupe mosquito quaranja-like virus 1 (previously described), referred to here as the Asto-Ūsinis clade within quaranjaviruses, did not resemble anything on GenBank via protein BLAST but were all inferred to strongly resemble gp64 proteins via HHpred and as such were aligned using MAFFT in G-INS-i mode.

The PB1 dataset was then reduced to viruses for which gp64 sequences were largely available, members of the Asto-Ūsinis clade, and more diverged members.

Phylogenetic trees for both PB1 and gp64 proteins were inferred using PhyML v.3.3.2 and rooted on isavirus for PB1 sequences and depicted unrooted for gp64.

For each PB1 blast hit we searched GenBank for the rest of the genome, ignoring any genomes that appear to have fewer than 6 segments on account of the three RdRp segments, nucleoprotein and occasionally surface proteins being far easier to identify and all of the best-studied orthomyxoviruses having at least six segments. We visualized PB1 and gp64 trees using baltic and annotated tips with number of segments identified and category of surface protein used, where available. For annotating genome organization we further marked the earliest plausible common ancestors that must have possessed a given genome organization and highlighted all of their descendants as a prediction for which other datasets might have the missing segments.

3.3 Phylogenetic diversity estimation

The larger PB1 sequence data set (prior to reduction) was used to infer a maximum likelihood tree using PhyML v.3.3.2 which was rooted on isaviruses. For each protein, the date of either its publication in literature or on GenBank was noted. For each year of discovery available, tree branches were marked with the evolutionary path uncovered that year, starting from oldest published sequences. The sum of branch lengths contributed by any given sequence to the tree is what we call phylogenetic diversity (PD). As well as the relationship between year of discovery and maximum PD contributed in Fig. 3A we looked at successive and unique PD contributions by each newly discovered orthomyxovirus in comparison to a neutral PD discovery curve.

3.4 Data availability

Data and scripts to replicate analyses are publicly available at `https://github.com/evogytis/orthomyxo-metagenomics`.

4 Acknowledgements

We would like to acknowledge the contributions of Amy Kistler, Maira Phelps, Cristina Tato, and Fabiano Oliveira in setting up sample logistics, experimental design, and data analysis for the Californian mosquito virome study. We would like to thank Darren Obbard for numerous and fruitful discussions. We are grateful to Jessica Manning, Dara Kong, Sreyngim Lay, Alex Greninger, Mang Shi, Eddie C Holmes, Dana Price, and John Pettersson for sharing assembled sequence data.

References

Allison AB, Ballard JR, Tesh RB, et al. (18 co-authors). 2015. Cyclic Avian Mass Mortality in the Northeastern United States Is Associated with a Novel Orthomyxovirus. *Journal of Virology*. 89:1389–1403.

Altschul SF, Gish W, Miller W, Myers EW, Lipman DJ. 1990. Basic local alignment search tool. *Journal of Molecular Biology*. 215:403–410.

Arunkumar GA, Bhavsar D, Li T, et al. (13 co-authors). 2021. Functionality of the putative surface glycoproteins of the Wuhan spiny eel influenza virus. *Nature Communications*. 12:6161. Number: 1 Publisher: Nature Publishing Group.

Baker SF, Nogales A, Finch C, Tuffy KM, Domm W, Perez DR, Topham DJ, Martínez-Sobrido L. 2014. Influenza A and B Virus Intertypic Reassortment

through Compatible Viral Packaging Signals. *Journal of Virology*. 88:10778–10791. Publisher: American Society for Microbiology Journals Section: Structure and Assembly.

Bataille A, Cunningham AA, Cedeño V, et al. (11 co-authors). 2009. Evidence for regular ongoing introductions of mosquito disease vectors into the Galápagos Islands. *Proceedings of the Royal Society B: Biological Sciences*. 276:3769–3775. Publisher: Royal Society.

Batson J, Dudas G, Haas-Stapleton E, Kistler AL, Li LM, Logan P, Ratnasiri K, Retallack H. 2021. Single mosquito metatranscriptomics identifies vectors, emerging pathogens and reservoirs in one assay. *eLife*. 10:e68353. Publisher: eLife Sciences Publications, Ltd.

Batts WN, LaPatra SE, Katona R, et al. (12 co-authors). 2017. Molecular characterization of a novel orthomyxovirus from rainbow and steelhead trout (Oncorhynchus mykiss). *Virus Research*. 230:38–49.

Bedford T, Cobey S, Pascual M. 2011. Strength and tempo of selection revealed in viral gene genealogies. *BMC Evolutionary Biology*. 11:1–16. Number: 1 Publisher: BioMed Central.

Bouckaert R, Vaughan TG, Barido-Sottani J, et al. (25 co-authors). 2019. BEAST 2.5: An advanced software platform for Bayesian evolutionary analysis. *PLOS Computational Biology*. 15:e1006650.

Chare ER, Gould EA, Holmes EC. 2003. Phylogenetic analysis reveals a low rate of homologous recombination in negative-sense RNA viruses. *Journal of General Virology*. 84:2691–2703.

Di Giallonardo F, Geoghegan JL, Docherty DE, et al. (12 co-authors). 2015. Fluid Spatial Dynamics of West Nile Virus in the United States: Rapid Spread in a Permissive Host Environment. *Journal of Virology*. 90:862–872. Publisher: American Society for Microbiology.

Drummond AJ, Pybus OG, Rambaut A, Forsberg R, Rodrigo AG. 2003. Measurably evolving populations. *Trends in Ecology & Evolution*. 18:481–488.

Felsenstein J. 1985. Phylogenies and the Comparative Method. *The American Naturalist*. 125:1–15. Publisher: [University of Chicago Press, American Society of Naturalists].

Finn RD, Clements J, Eddy SR. 2011. HMMER web server: interactive sequence similarity searching. *Nucleic Acids Research*. 39:W29–W37.

Fonseca DM, Smith JL, Wilkerson RC, Fleischer RC. 2006. PATHWAYS OF EXPANSION AND MULTIPLE INTRODUCTIONS ILLUSTRATED BY LARGE GENETIC DIFFERENTIATION AMONG WORLDWIDE POPULATIONS OF THE SOUTHERN HOUSE MOSQUITO. *The American Journal of Tropical Medicine and Hygiene*. 74:284–289. Publisher: The American Society of Tropical Medicine and Hygiene.

Frey KG, Biser T, Hamilton T, Santos CJ, Pimentel G, Mokashi VP, Bishop-Lilly KA. 2016. Bioinformatic Characterization of Mosquito Viromes within the Eastern United States and Puerto Rico: Discovery of Novel Viruses. *Evolutionary Bioinformatics Online*. 12:1–12.

Garry CE, Garry RF. 2008. Proteomics computational analyses suggest that baculovirus GP64 superfamily proteins are class III penetrenes. *Virology Journal*. 5:28.

Ge XY, Wang N, Zhang W, et al. (14 co-authors). 2016. Coexistence of multiple coronaviruses in several bat colonies in an abandoned mineshaft. *Virologica Sinica*. 31:31–40.

Hasegawa M, Kishino H, Yano Ta. 1985. Dating of the human-ape splitting by a molecular clock of mitochondrial DNA. *Journal of Molecular Evolution*. 22:160–174.

He X, Yin Q, Zhou L, et al. (22 co-authors). 2021. Metagenomic sequencing reveals viral abundance and diversity in mosquitoes from the Shaanxi-Gansu-Ningxia region, China. *PLOS Neglected Tropical Diseases*. 15:e0009381. Publisher: Public Library of Science.

Huestis DL, Dao A, Diallo M, et al. (22 co-authors). 2019. Windborne long-distance migration of malaria mosquitoes in the Sahel. *Nature*. 574:404–408.

Hunter JD. 2007. Matplotlib: A 2D Graphics Environment. *Computing in Science Engineering*. 9:90–95. Conference Name: Computing in Science Engineering.

Jong JCd, Smith DJ, Lapedes AS, et al. (11 co-authors). 2007. Antigenic and Genetic Evolution of Swine Influenza A (H3N2) Viruses in Europe. *Journal of Virology*. 81:4315–4322. Publisher: American Society for Microbiology Journals Section: GENETIC DIVERSITY AND EVOLUTION.

Katoh K, Kuma Ki, Toh H, Miyata T. 2005. MAFFT version 5: improvement in accuracy of multiple sequence alignment. *Nucleic Acids Research*. 33:511–518.

Ke R, Aaskov J, Holmes EC, Lloyd-Smith JO. 2013. Phylodynamic Analysis of the Emergence and Epidemiological Impact of Transmissible Defective Dengue Viruses. *PLoS Pathogens*. 9. Publisher: Public Library of Science.

Keele BF, Van Heuverswyn F, Li Y, et al. (19 co-authors). 2006. Chimpanzee Reservoirs of Pandemic and Nonpandemic HIV-1. *Science*. 313:523–526. Publisher: American Association for the Advancement of Science.

Kistler KE, Bedford T. 2021. Evidence for adaptive evolution in the receptor-binding domain of seasonal coronaviruses OC43 and 229e. *eLife*. 10:e64509. Publisher: eLife Sciences Publications, Ltd.

Kobayashi M, Toyoda T, Ishihama A. 1996. Influenza virus PB1 protein is the minimal and essential subunit of RNA polymerase. *Archives of Virology*. 141:525–539.

Kondo H, Maeda T, Shirako Y, Tamada T. 2006. Orchid fleck virus is a rhabdovirus with an unusual bipartite genome. *Journal of General Virology,*. 87:2413–2421. Publisher: Microbiology Society,.

Konstantinidis K, Dovrolis N, Kouvela A, Kassela K, Freitas MGR, Nearchou A, Williams MdC, Veletza S, Karakasiliotis I. 2021. Defining Virus-Carrier Networks That Shape the Composition of the Mosquito Core Virome of an Ecosystem. preprint, In Review.

Koonin EV, Dolja VV. 2014. Virus World as an Evolutionary Network of Viruses and Capsidless Selfish Elements. *Microbiology and Molecular Biology Reviews*. 78:278–303. Publisher: American Society for Microbiology Section: Review.

Lemey P, Minin VN, Bielejec F, Pond SLK, Suchard MA. 2012. A counting renaissance: combining stochastic mapping and empirical Bayes to quickly detect amino acid sites under positive selection. *Bioinformatics*. 28:3248–3256.

Li CX, Shi M, Tian JH, Lin XD, Kang YJ, Chen LJ, Qin XC, Xu J, Holmes EC, Zhang YZ. 2015. Unprecedented genomic diversity of RNA viruses in arthropods reveals the ancestry of negative-sense RNA viruses. *eLife*. 4:e05378.

Li H, Durbin R. 2009. Fast and accurate short read alignment with Burrows–Wheeler transform. *Bioinformatics*. 25:1754–1760.

Li Z, Fan Y, Wei J, et al. (13 co-authors). 2019. Baculovirus Utilizes Cholesterol Transporter NIEMANN–Pick C1 for Host Cell Entry. *Frontiers in Microbiology*. 10.

Lounibos LP. 2002. Invasions by Insect Vectors of Human Disease. *Annual Review of Entomology*. 47:233–266. _eprint: https://doi.org/10.1146/annurev.ento.47.091201.145206

Lum D, Rheindt FE, Chisholm RA. 2022. Tracking scientific discovery of avian phylogenetic diversity over 250 years. *Proceedings of the Royal Society B: Biological Sciences*. 289:20220088. Publisher: Royal Society.

Lycett SJ, Duchatel F, Digard P. 2019. A brief history of bird flu. *Philosophical Transactions of the Royal Society B: Biological Sciences*. 374:20180257. Publisher: Royal Society.

Müller NF, Stolz U, Dudas G, Stadler T, Vaughan TG. 2020. Bayesian inference of reassortment networks reveals fitness benefits of reassortment in human influenza viruses. *Proceedings of the National Academy of Sciences*. 117:17104–17111. Publisher: National Academy of Sciences Section: Biological Sciences.

Park D, Dudas G, Wohl S, et al. (86 co-authors). 2015. Ebola Virus Epidemiology, Transmission, and Evolution during Seven Months in Sierra Leone. *Cell*. 161:1516–1526.

Parry R, Wille M, Turnbull OMH, Geoghegan JL, Holmes EC. 2020. Divergent Influenza-Like Viruses of Amphibians and Fish Support an Ancient Evolutionary Association. *Viruses*. 12:1042. Number: 9 Publisher: Multidisciplinary Digital Publishing Institute.

Pettersson JHO, Shi M, Eden JS, Holmes EC, Hesson JC. 2019. Meta-Transcriptomic Comparison of the RNA Viromes of the Mosquito Vectors Culex pipiens and Culex torrentium in Northern Europe. *Viruses*. 11.

Qin XC, Shi M, Tian JH, et al. (15 co-authors). 2014. A tick-borne segmented RNA virus contains genome segments derived from unsegmented viral ancestors. *Proceedings of the National Academy of Sciences*. 111:6744–6749. ISBN: 9781324194118 Publisher: National Academy of Sciences Section: Biological Sciences.

Rambaut A, Drummond AJ, Xie D, Baele G, Suchard MA. 2018. Posterior Summarization in Bayesian Phylogenetics Using Tracer 1.7. *Systematic Biology*. 67:901–904.

Roux S, Matthijnssens J, Dutilh BE. 2021. Metagenomics in Virology. *Encyclopedia of Virology*. pp. 133–140.

Sagulenko P, Puller V, Neher RA. 2018. TreeTime: Maximum-likelihood phylodynamic analysis. *Virus Evolution*. 4.

Shi C, Beller L, Deboutte W, Yinda KC, Delang L, Vega-Rúa A, Failloux AB, Matthijnssens J. 2019. Stable distinct core eukaryotic viromes in different mosquito species from Guadeloupe, using single mosquito viral metagenomics. *Microbiome*. 7:121.

Shi M, Lin XD, Chen X, et al. (12 co-authors). 2018. The evolutionary his-

tory of vertebrate RNA viruses. *Nature*. 556:197.

Shi M, Neville P, Nicholson J, Eden JS, Imrie A, Holmes EC. 2017. High-Resolution Metatranscriptomics Reveals the Ecological Dynamics of Mosquito-Associated RNA Viruses in Western Australia. *Journal of Virology*. 91.

Suchard MA, Lemey P, Baele G, Ayres DL, Drummond AJ, Rambaut A. 2018. Bayesian phylogenetic and phylodynamic data integration using BEAST 1.10. *Virus Evolution*. 4.

Wang ZD, Wang B, Wei F, et al. (22 co-authors). 2019. A New Segmented Virus Associated with Human Febrile Illness in China. *New England Journal of Medicine*. 380:2116–2125.

Webster CL, Waldron FM, Robertson S, et al. (14 co-authors). 2015. The Discovery, Distribution, and Evolution of Viruses Associated with Drosophila melanogaster. *PLoS Biology*. 13.

Wheeler DC, Waller LA, Biek R. 2010. Spatial analysis of feline immunodeficiency virus infection in cougars. *Spatial and Spatio-temporal Epidemiology*. 1:151–161.

Whitfield ZJ, Dolan PT, Kunitomi M, Tassetto M, Seetin MG, Oh S, Heiner C, Paxinos E, Andino R. 2017. The Diversity, Structure, and Function of Heritable Adaptive Immunity Sequences in the Aedes aegypti Genome. *Current Biology*. 27:3511–3519.e7.

Wu F, Zhao S, Yu B, et al. (19 co-authors). 2020. A new coronavirus associated with human respiratory disease in China. *Nature*. 579:265–269. Number: 7798 Publisher: Nature Publishing Group.

Yang Z. 1994. Maximum likelihood phylogenetic estimation from DNA sequences with variable rates over sites: Approximate methods. *Journal of Molecular Evolution*. 39:306–314.

5 Supplementary material

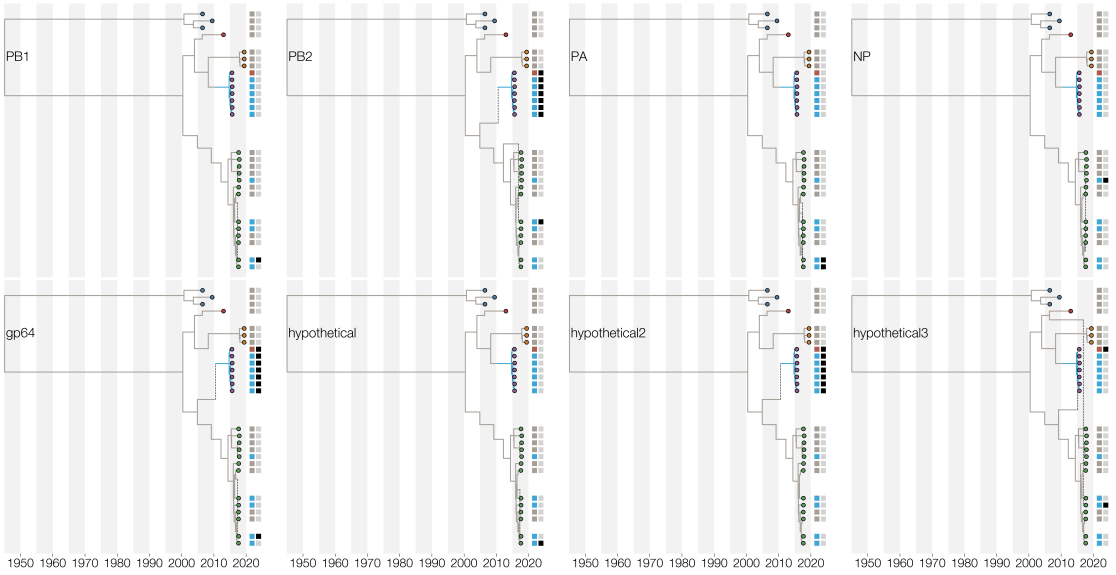

Figure S1. Segment paths through the reassortment network. Each panel shows the embedding of every segment in the reassortment network of Wuhan mosquito virus 6 genomes. Tips are colored by location, as in Figure 1A in the main text. The first colored box to the right of the tree indicates how many successive reassortments the entire genome a tip belongs to has experienced reassortment - cycling between grey, blue, and brown colors for each successive event. The second colored box indicates whether the segment in question has undergone a reassortment event.

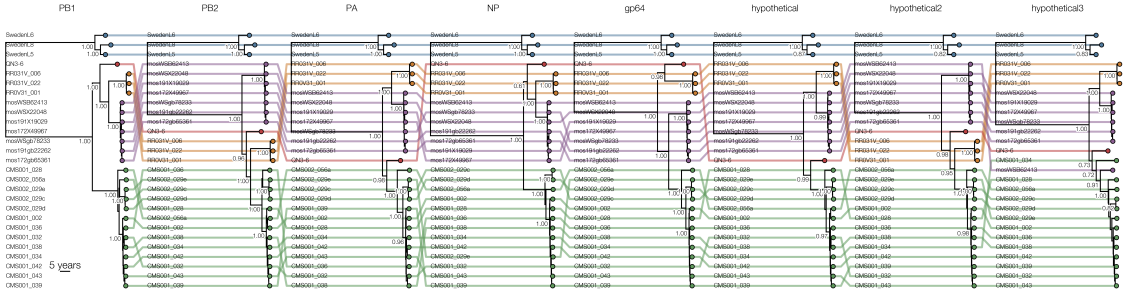

Figure S2. Tangled chain of maximum clade credibility trees of individual segment embeddings. Each tree corresponds to a segment of Wuhan mosquito virus 6, with tips colored the same as Fig. 1 in the main text. The same tips are connected with colored lines between successive trees to indicate changes in their phylogenetic position, their names are given at the base of each tree. Numbers at each internal branch longer than 1.0 year correspond to the node's posterior probability.

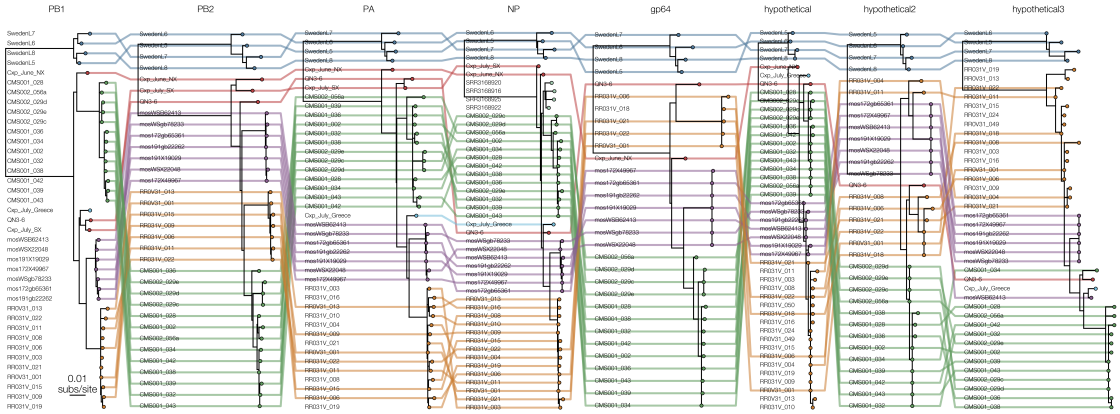

Figure S3. Tangled chain of maximum likelihood trees of individual segments. Each tree corresponds to all available segments of Wuhan mosquito virus 6, with tips colored the same as Figure 1A in the main text. The same tips are connected with colored lines between successive trees (if the corresponding segment was identified for that genome) to indicate changes in their phylogenetic position, their names are given at the base of each tree. Unlike Supp. Fig. 2, samples from Puerto Rico, Greece, Cambodia, and additional Chinese sequences are included here.

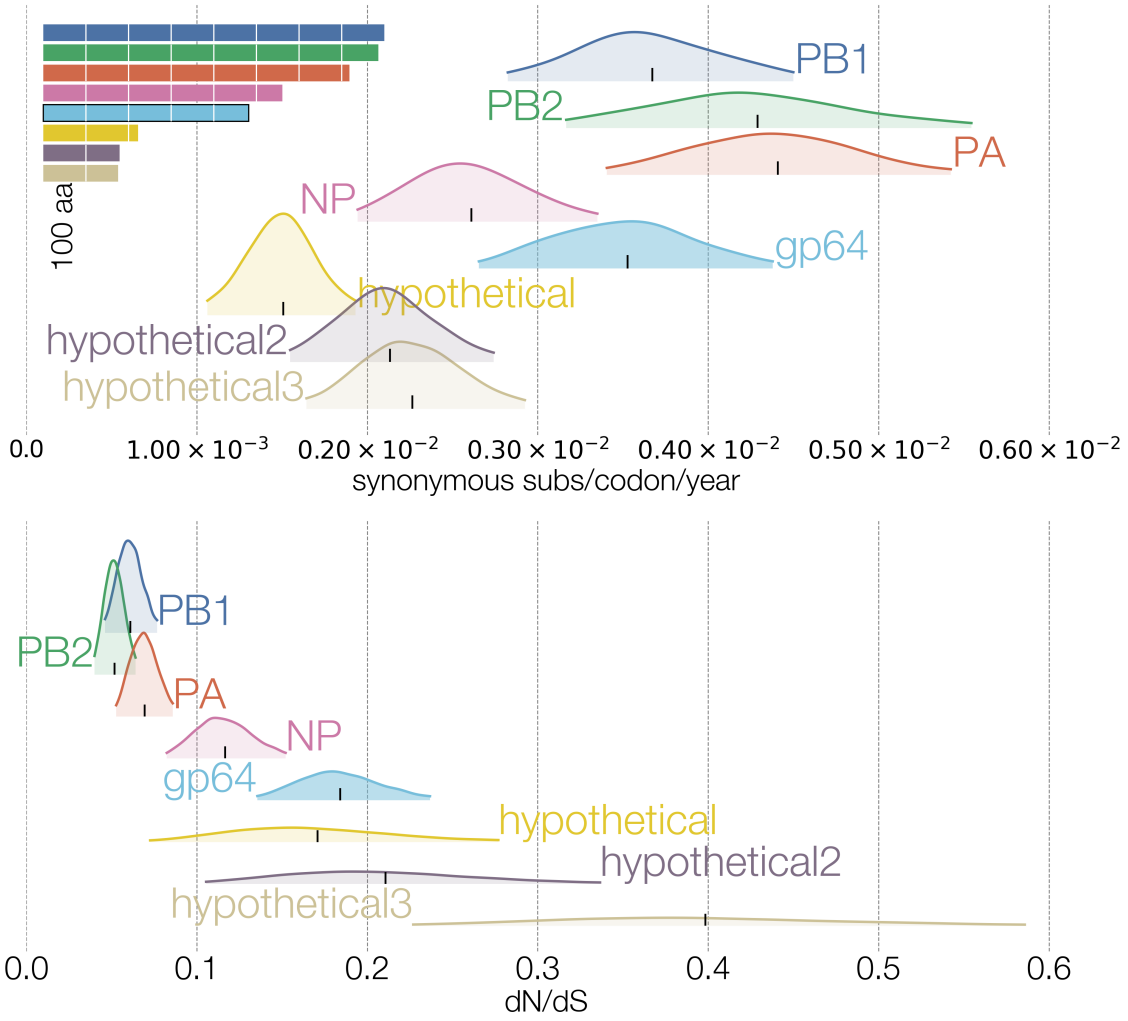

Figure S4. Estimates of synonymous rate of evolution and dN/dS for Wuhan mosquito virus 6 genes. The top panel shows 95% highest posterior densities of the synonymous rate of evolution for each WMV6 gene (distinguished by color). Colored rectangles in the top left show the relative lengths of each gene with white lines indicating 100 amino acid increments. The bottom panel shows 95% highest posterior densities of dN/dS for each WMV6 gene.

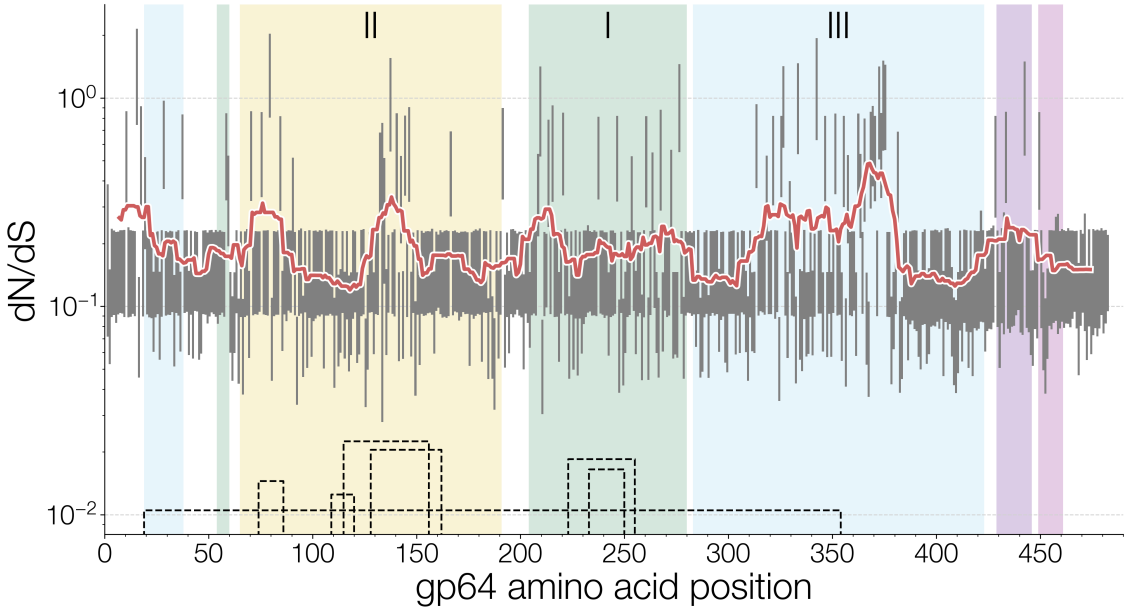

Figure S5. Estimates of dN/dS in gp64 per codon. Grey vertical lines indicate the 95% highest posterior density interval for dN/dS per codon in gp64 of Wuhan mosquito virus 6. The red line tracks mean estimated dN/dS in a sliding window of 15 amino acids. Regions of the protein are colored and labelled according to nomenclature proposed by Garry and Garry (2008). Dashed lines at the bottom depict putative disulfide bonds between cysteins in gp64, based on Garry and Garry (2008). The two peaks in average dN/dS in domain II occupy predicted regions of thogotovirus gp64 fusion loops which are inserted into the target membrane. A notable region of elevated dN/dS is seen in domain III but is difficult to explain since the region is expected to be proximal to the viral, and not the host, membrane.

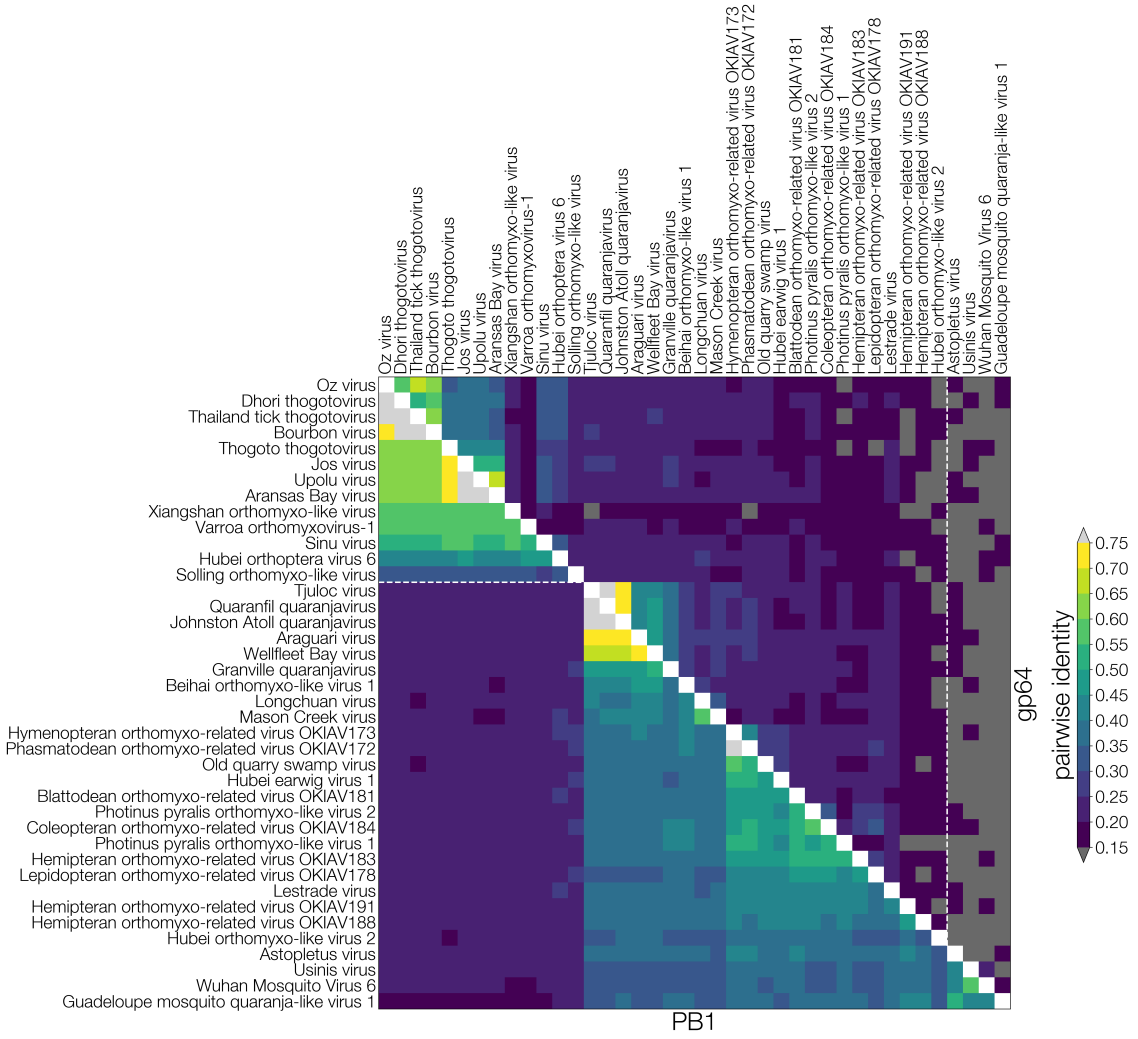

Figure S6. Pairwise distance matrix between PB1 (lower triangle) and gp64 (upper triangle) proteins. Dashed horizontal line marks the difference in PB1 between thogoto-like (above) and quaranja-like (below) viruses. Dashed vertical line marks the difference between stereotypically quaranjavirus (to the left) and the markedly diverged quaranja-like gp64 proteins used by the eight-segmented Asto-Ūsinis clade (to the right).

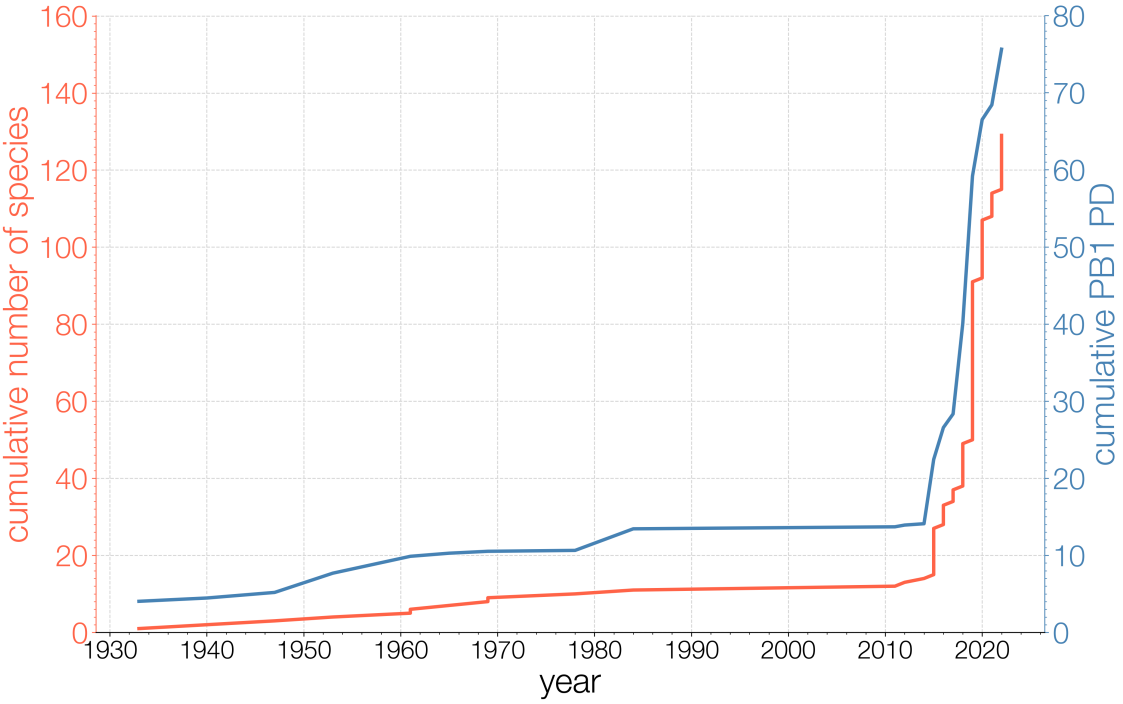

Figure S7. Orthomyxovirus species (red) and PB1 phylogenetic diversity (blue) discovery curves. Regardless of whether discovery efforts are quantified in terms of raw species numbers or phylogenetic diversity, 2015 has marked a major turning point for discovery of orthomyxo- and other RNA viruses.